Fourier optical limits of coherent acousto-optic matrix-vector processor

Thomas J. Naughton

Department of Computer Science, National University of Ireland/Maynooth, Maynooth, Ireland

ABSTRACT

We characterize the bounds on numerical accuracy that a finite acoustic beam height will have on an analog acousto-optic algebra processor that uses coherent illumination. A Fourier optical model of our physical matrix-vector multiplier is used as a basis for the simulations.

Keywords: optical information processing, physical limits of optics in computing, optical matrix-vector systems, acousto-optical signal processing, Fourier optics, analog optical computing, spatial filtering

1. INTRODUCTION

A number of important research efforts have quantified the errors associated with various analog optical processors,[1–6] including AO algebra processors. These analyses have looked at AO cell characteristics such as frequency response and acoustic attenuation, addressed overheads associated with digital numbering systems, and employed statistical noise models to quantify errors. We consider analog algebra processors that use coherent illumination. A spatially integrating acousto-optic (AO) matrix-vector processor has been built and has already been used to train a simple artificial neural network.[7] In this paper, we investigate the restrictions that a finite acoustic beam height will have on its numerical calculation abilities. The spatial filtering effects of finite-dimension devices in coherent optical systems are known; we determine to what degree it impedes scaling of the architecture.

We have derived a Fourier model of the coherent AO matrix-vector multiplier (MVM) and use it to examine the relationship between numerical accuracy and acoustic beam height. We find that the spatial filtering effects result in the detection of a blurred matrix-vector product. This relationship is important to characterize; the spatial filtering effects will become more pronounced as the resolution of the matrix SLM is scaled upwards. A novel representation of the input plane signal allows us to simulate the combined diffraction pattern of an arbitrary SLM pixel structure and arbitrary matrix data. We can also incorporate images of the acoustic beam in the event that inhomogeneities or nonlinear absorption prevent an analytical description of the acoustic propagation.

For a given acoustic beam height (and given illumination, lens configuration, and so on) we also quantify how much inter-row unused spacing must be added to the matrix as the SLM resolution increases. The model has been verified experimentally using a 2-D CCD camera (simulating a 1-D sensor of arbitrary pixel aspect ratio) and a computer-controlled LCD (liquid crystal display) panel. Although we are very specific in our choice of architecture, AO cells and LCD panels, the results should be applicable to any coherent optical system. In Sect. 2 we describe our AO MVM and give the Fourier optical model of its operation. We next outline a discrete computational theory describing how a Fourier transform (FT) processor can approximate a matrix-vector multiplication. In Sect. 3 we describe a lookup table system to ensure linear summation under coherent illumination. Section 4 combines our Fourier and computational theories in a series of experiments to analyze the numerical accuracy of coherent AO algebra processors as they are scaled upwards (or as the level of filtering increases).

2. AO MVM

In our matrix-vector processor the matrix of weights is displayed on a 2-D LCD panel and the input vector is encoded in the acoustic wave of an AO unit (AOU). Its operation can be visualized from the schematic in Fig. 1. Using optical components, each row of the matrix is directed through, and is thus multiplied by, the vector encoded in the second SLM. Summing the resulting values in each row produces a vector representing the inner matrix-vector product. The implementation of our space-integrating[8] AO processor can be seen schematically in Fig. 2. As

Further author information. Fax: +353-1-7083848 Email: tomn@cs.may.ie

shown, the collimated beam from the laser is first expanded. The beam expander consists of lenses L1 and L2 and has an expansion ratio of 1:50. In the vertical direction (side view), cylindrical lens L3 operates as a Fourier lens in the standard 1-f setup, such that the matrix columns are Fourier transformed at L3's focal plane. The AOU's acoustic beam is centered along this plane so that it coincides with the zero-order of the LCD image's 1-D FT. In the horizontal direction (top view in Fig. 2), lens L3 does not influence the laser beam. The input vector is encoded in the acoustic wave of the AOU, which operates in the Bragg regime. As a result, the first AO diffracted order (given sufficient time and space to spatially expand) is a 2-D signal containing the multiplication of the matrix coefficients from each row of the LCD and this input vector. The row summation and imaging on the detector is performed by lenses L4 and L5 and the sampled vector interfaced to a PC. The matrix and vector values are also controlled by a computer program executing on a PC. By extracting a predefined pattern of pixels from our 2-D CCD image we can simulate a 1-D detector of arbitrary width.

2.1. Fourier Optical Model

Coherent optical systems are straightforward to analyze since they can be approximated using the equations of Fourier optics. If we ignore scaling factors due to lens configurations and let (x, y) describe each space domain and (α, β) describe each frequency domain along our optical system, the detected output signal s_{DET} can be written as

$$s_{\text{DET}}(\alpha, -y) = \left| C(\alpha) \iint_{-\infty}^{\infty} \left[A(\beta) g(x) \int_{-\infty}^{\infty} f(x, y) \exp(i 2\pi \beta y) \mathrm{d}y \right] \times \exp[i 2\pi(\alpha x + \beta y)] \mathrm{d}x \mathrm{d}\beta \right|^2 , \quad (1)$$

where f is the LCD panel signal and g is the signal encoded in the acoustic beam. The 1-D signal A is a binary-valued spatial frequency bandpass filter, infinite in the x-direction, which corresponds to the height of the acoustic beam along its length. We presume that the acoustic beam undergoes negligible absorption and divergence. If such divergence is to be modeled, then a (possibly real-valued) 2-D filter should be used for A. Finally, C is a binary-valued 1-D spatial frequency bandpass filter, infinite in the y-direction, which corresponds to the width of the linear CCD sensor.

2.2. Discrete computational model

Ignoring filtering effects, we are multiplying the FT of each column of matrix f by an element of vector g. This can be written as

$$s(-y) = \sum_x f(x, y) \star G_y(x, 0) \ , \quad (2)$$

where $\star$ is a 1-D vertical convolution operator and $G_y(x, \beta)$ is how we might regard a vertical 1-D FT of horizontal vector $g(x)$. According to the relationship between a δ-function and its FT and employing the conservation of energy theorem, we can say $g(x, y) \approx G_y(x, 0)$ for every x when $g(x, y)$ is constant valued in the y-direction (i.e. independent of y). Since convolution with a scalar is a point-by-point multiplication, our coherent AO system approximates

$$s_{-y} \approx \sum_x f_{xy} g_x \ . \quad (3)$$

3. SUMMATION EXPERIMENTS

Summation with binary amplitude values is straightforward with coherent optics. This has allowed us in the past to successfully implement a Hough transform[7] for arbitrary shape detection that uses a binary representation of its input images. Additionally, to represent real (rational) values, we can use area modulation. This is achieved by using the LCD panel to represent a lower-resolution matrix of data values where each data value is encoded in a square of pixels. With squares of side N pixels, area modulation effectively allows $(N^2 + 1)$ resolvable levels in the range [0,1]. Employing area modulation, we can linearly sum real values on our AO MVM (as experimentally verified in Fig. 3) and this has enabled us to train a simple artificial neural network with real-valued weights.[7]

Different nonzero amplitude values will not be summed linearly in a coherent optical processor, however. This is illustrated through simulation and optical experiment in Fig. 4. (All simulations were performed with MATLAB from The Mathworks Inc.) In Fig. 4, our output should be a constant valued vector [i.e. $(5 + 1)$ should equal $(4 + 1 + 1)$]. Instead, we see a quadratic curved response. Such a nonlinear response is not a problem if it is repeatable. We find a lookup table approach works well.

3.1. Summation with lookup table

The curve we see in Fig. 4 indicates that the detector measures a quadratic function of each matrix value. This is to be expected from the square law for detectors and can be reasoned about in terms of constructive interference of coherent wavefronts. In order to compensate for this we apply a lookup table to our data in advance of writing to the LCD display. This lookup table substitutes each gray-level with a value corresponding to its square root. Figure 5 shows that rounding errors aside, this techniques produces a good approximation. For the remaining experiments, in order to concentrate on the other variables in our system, we assume that this lookup table approach is error free.

4. FILTERING EXPERIMENTS

In this set of experiments, we seek to determine the effect of a finite AO interaction height on row summation. This is important as it mirrors the effects on numerical accuracy of increasing LCD resolution. Under coherent illumination, the acoustic beam of an AO MVM acts as a bandpass filter on the Fourier spectrum of each matrix column. Figure 6 shows the effect of a finite AO interaction height on spatial resolution in the output plane. As less vertical spatial frequencies make it through the system, the separate horizontal spectra of the output signal (which correspond to individual summed rows of the matrix-vector point multiplication) become less distinguishable. The implications for numerical computations are obvious. An acoustic beam whose height is not sufficient to pass enough vertical spatial frequency information will cause the individual output vector data values to overlap in the detector plane.

In order to characterize the dependency between AO interaction height and MVM accuracy we perform filtering with several input matrices and a vector of 1's. Figures 7 through 9 show some results from these experiments for important classes of input matrix. We plot the values in the output vector against varying interaction height and also plot the resulting errors in each calculation. In Fig. 7(d) note the 'step' effect; the three orders in Fig. 7(b) are passed one by one as the interaction height is increased. Filtering at any of the horizontal linear regions will produce numerically accurate results (after subtraction of the appropriate offset). Two linear regions of interest are marked ROI1 and ROI2.

ROI1 represents the range of interaction heights between the optical axis and the first order of LCD grid diffraction. This is where most of the spatial frequency information of the input matrix will appear. ROI1 is plotted in more detail in Fig. 7(f). In order to ensure accuracy in the matrix-vector calculation, over all possible input matrices, we require the edge of our acoustic beam to be in such a stable region. The 'steps' are fixed by the LCD's sampling frequency; we can therefore determine some useful quantitative limits relative to these orders. For the matrix used in Fig. 7, an acoustic beam that intersects no less than 25% $\left(\frac{7\times0.01}{7\times0.04}\right)$ of the spatial frequencies between the zeroth and first LCD diffracted order will correctly sum the partial products. The uncertainty in the calculation can also be calculated from the graph. ROI2 represents a range of interaction heights between the first and second LCD grid diffraction orders. It is also stable for this matrix. In Fig. 8, for a matrix that uses the full space-bandwidth product of the LCD panel, region ROI1 has become less stable, and in Fig. 9 for matrices that happen to contain only binary values, ROI1 is unusable. In all cases, the closest stable region to the optical axis is ROI2. This means that the minimum interaction height that has a boundary in a stable region includes all of the LCD grid's first diffraction order.

Standard procedure when positioning an AOU in the back Fourier plane of the matrix SLM tries to include all frequencies between the zeroth and first LCD diffraction order. These results show that to ensure numerical accuracy (linear summing of matrix row information) it is essential to pass all frequencies up to and including the first diffracted order of the LCD panel. This affects the scalability of coherent optical matrix-vector systems that combine LCD panels with AOUs. For a given AOU (and given focal length lenses, illumination, and so on) there is a maximum matrix SLM bandwidth. If exceeded, the Fourier spectrum in the AO plane will be too large to be passed by the AOU. If the AO interaction height cannot be changed, then a new Fourier lens configuration to

rescale the frequency spectrum or a spatial separation of the inputs in the LCD plane could be tried. We consider the latter option next.

4.1. Spatial separation of matrix information

The acoustic beam height of an AOU cannot easily be changed. In situations where it is not sufficient, and blurring occurs as shown in Fig. 6, inter-row spacing on the LCD panel has been suggested as a technique to spatially separate the elements of the vector in the output plane. However, a fixed spatial filter in the form of the AOU means a fixed lower bound on the resolution of matrix information that will be allowed to pass. There turns out to be a linear relationship between increased resolution and amount of inter-row spacing required for a fixed acoustic beam height. Simulations with our model in Fig. 10 illustrate this finding.

5. CONCLUSION

Our Fourier model of a coherent AO MVM can be used to examine the relationship between numerical accuracy and acoustic beam height. We see from these experiments that the limitations of a finite acoustic beam height are extremely important considerations when implementing a coherent AO MVM. Numerical accuracy can only be assured when spatial frequency information up to and including the first diffracted order from the LCD panel is allowed to pass. For a fixed acoustic beam height, any space-bandwidth product gains obtained by increasing the resolution of the LCD will be lost by the requirement for additional inter-row spacing to preserve numerical accuracy. Fourier spectrum size reduction techniques (varying focal length, cascaded Fourier transformation, varying SLM-lens spacing) can alleviate the situation, but as the matrix SLM is miniaturized or increases resolution the problems return.

The next stage of this work will involve incorporating the effects of a finite detector width into the simulation and determining the optimal sensor aspect ratio given predefined parameters of the AO system.

ACKNOWLEDGMENTS

Many thanks to the Department of Computer Science, NUI Maynooth, and especially to Head of Department, Stephen Brown, for financial assistance.

REFERENCES

1. S. G. Batsell, T.-L. Jong, J. F. Walkup, and T. F. Krile, "Noise limitations in optical linear algebra processors," *Applied Optics* **29**, pp. 2084–2090, May 1990.
2. D. P. Casasent and A. K. Ghosh, "Optical linear algebra processors: noise and error-source modeling," *Optics Letters* **10**, pp. 252–254, June 1985.
3. A. K. Ghosh, D. P. Casasent, and C. P. Neuman, "Performance of direct and iterative algorithms on an optical systolic processor," *Applied Optics* **24**, pp. 3883–3892, Nov. 1985.
4. Y. Li and B. Ha, "How large can an optical matrix-matrix multiplier be constructed?," in *Advances in Optical Information Processing VI*, D. R. Pape, ed., Proceedings of SPIE vol. 2240, pp. 132–143, (Orlando, Florida), Apr. 1994.
5. D. Psaltis and R. A. Athale, "High accuracy computation with linear analog optical systems: a critical study," *Applied Optics* **25**, pp. 3071–3077, Sept. 1986.
6. C. W. Stirk, "Bit error rate of optical logic: fan-in, threshold, and contrast," *Applied Optics* **31**, pp. 5632–5641, Sept. 1992.
7. T. Naughton, Z. Javadpour, J. Keating, M. Klíma, and J. Rott, "General-purpose acousto-optic connectionist processor," *Optical Engineering* **38**, pp. 1170–1177, July 1999.
8. A. VanderLugt, *Optical Signal Processing*, Wiley Series in Pure and Applied Optics, Wiley, New York, 1992.

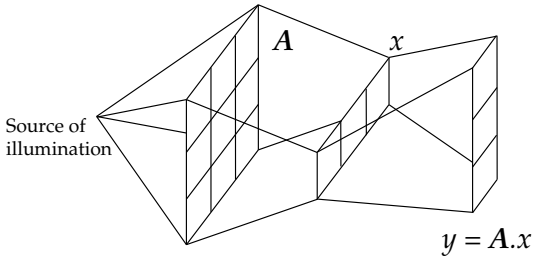

Figure 1. Space-integrating AO MVM.

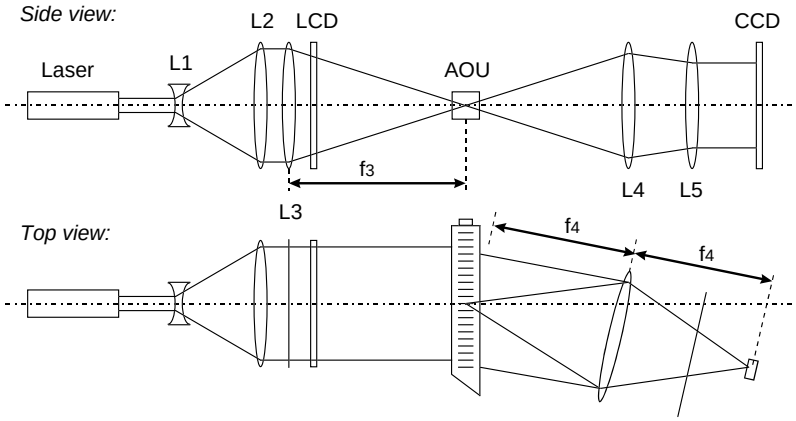

Figure 2. Schematic of the optical setup: LCD, matrix spatial light modulator; AOU, AO unit encoding a vector; CCD, detector; and L3, L5, cylindrical lenses.

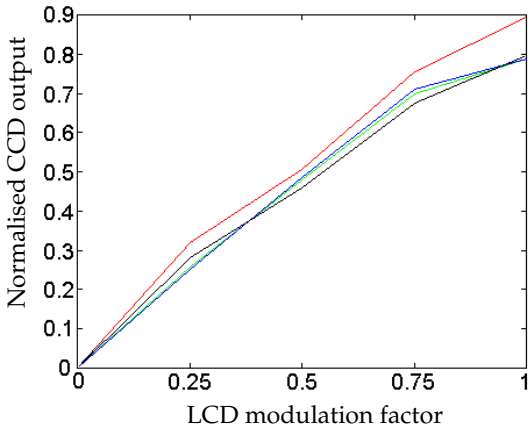

Figure 3. Output vectors corresponding to four rational-valued input matrices. Plots give an indication of the linearity of our physical AO MVM when it employs area modulation. The different matrices had values that meant they should produce identical products when multiplied by a vector of 1's. A simple vector subtraction to compensate for the Gaussian profile of the laser beam was performed before plotting.

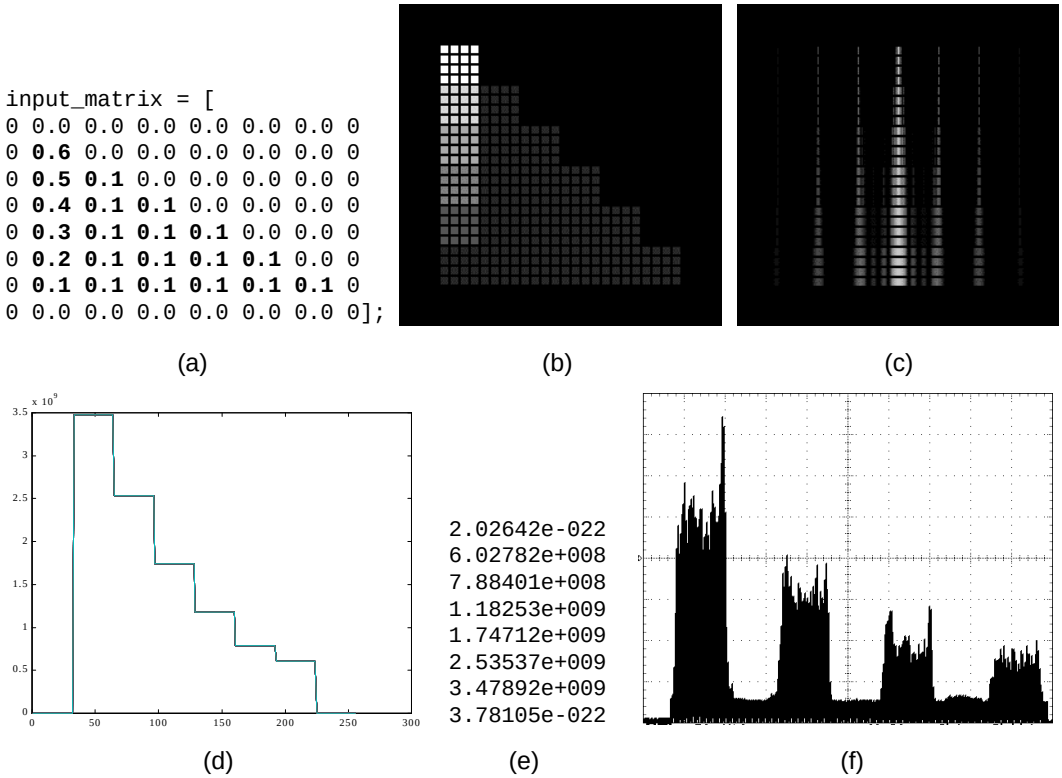

Figure 4. Quadratic response to summation. Values encoded by amplitude in a coherent wavefront are not summed linearly: (a) the real-valued input matrix that is to be multiplied by a vector of 1's; (b) simulation of the optical signal immediately behind an LCD panel encoding each matrix element as a gray level in a 4×4 pixel subgrid; (c) simulated output of the AO MVM (inverted); (d) plot of the output vector, the result of integrating (c) horizontally over all orders and binning into a vector of the same height as the matrix's width; (e) the actual values obtained for (d)'s plot; (f) output from a similar experiment on our physical AO system, also showing the quadratic response curve. No filtering was performed in these simulations.

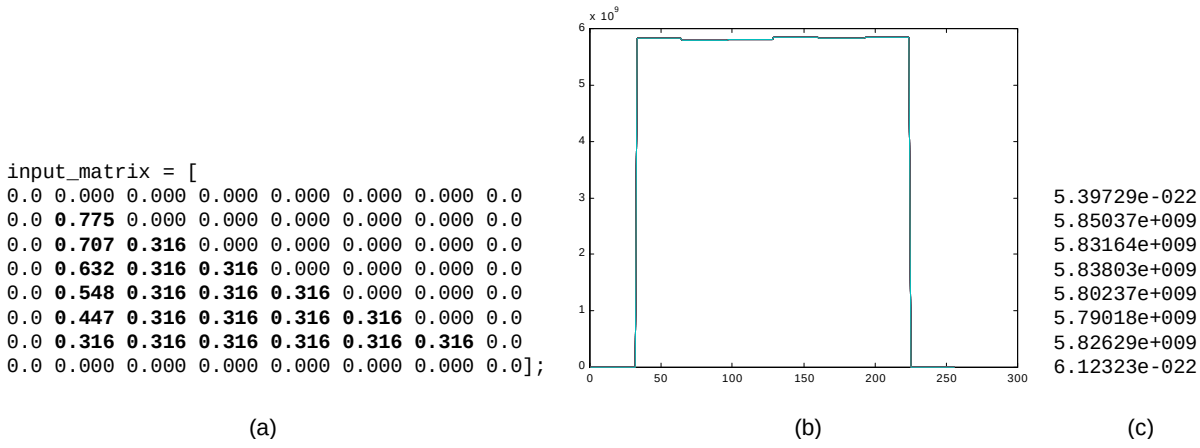

Figure 5. Employing a lookup table of square root values provides a good approximation to linear summation: (a) the result of applying the lookup table to Fig. 4(a); (b) plot of the simulated output vector; (c) values used to generate (b). Except for rounding errors due to a discrete allowable set of LCD gray levels, the vector is constant valued (thus verifying linearity).

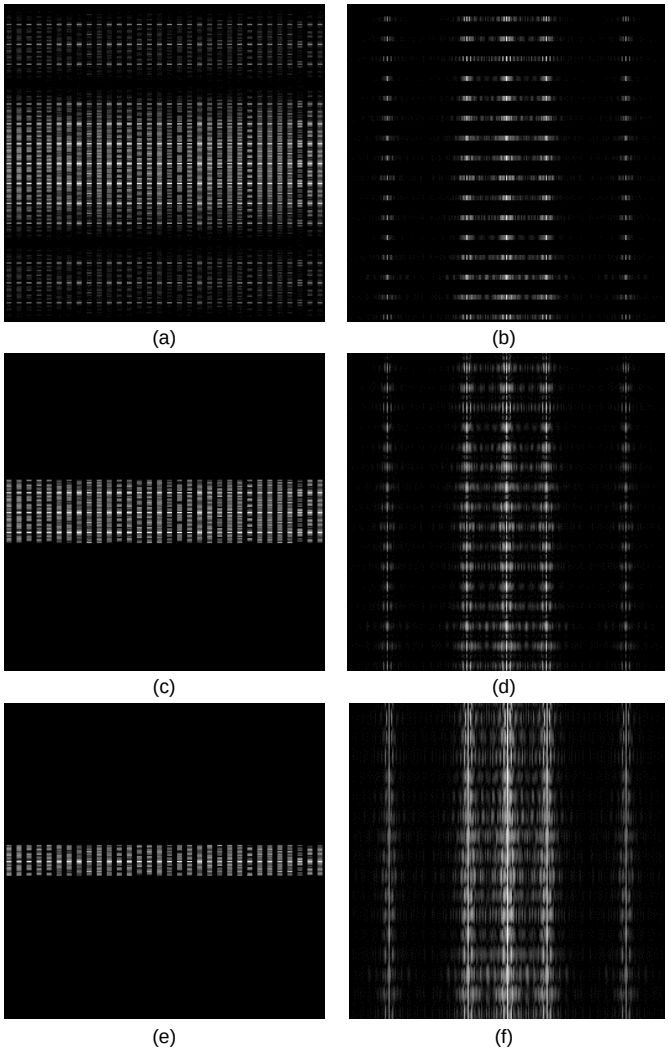

Figure 6. Effect of a finite AO interaction height on the output plane signal. Input signal is an image composed of rows of randomly distributed binary values separated by blank rows: (a) simulated unfiltered signal at the AO plane; (b) corresponding output plane signal showing clearly separated rows of information; (c) and (e) spatially filtered signals due to two different values for acoustic beam height; (d) and (f) their corresponding output plane signals.

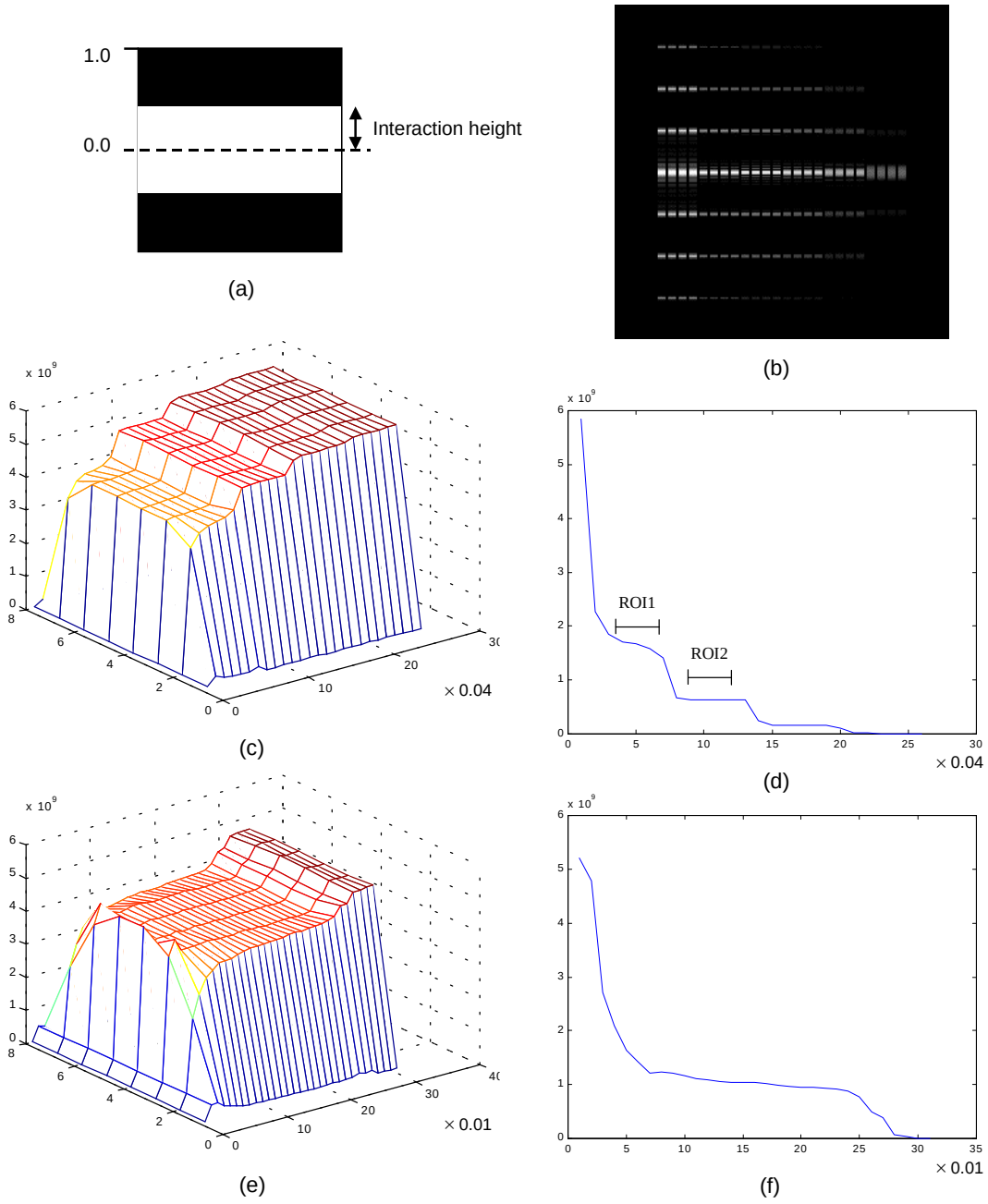

Figure 7. Degradation in summation accuracy due to AO plane filtering: (a) an illustration of the mask used to multiply AO plane signals. The mask, centered on the zeroth LCD diffracted order, combines a vector of 1's with an acoustic interaction height. Heights range from 0 (block all) to 1 (pass all); (b) the AO plane signal corresponding to the Fig. 5(a) input matrix. This complex image is filtered with the mask in (a) for various interaction heights; (c) plot of the numerical values in the 8×1 output vector against increasing interaction height. Heights are in the range $[0, 1]$ with graduations of 0.04 (labeled 1 to 26); (d) a plot of the highest individual error in each vector of (c); (e) as in (c), but restricted to interaction heights in the range $[0.0, 0.3]$ and with graduations of 0.01; (f) corresponding plot of the highest error in each of (e)'s output vectors.

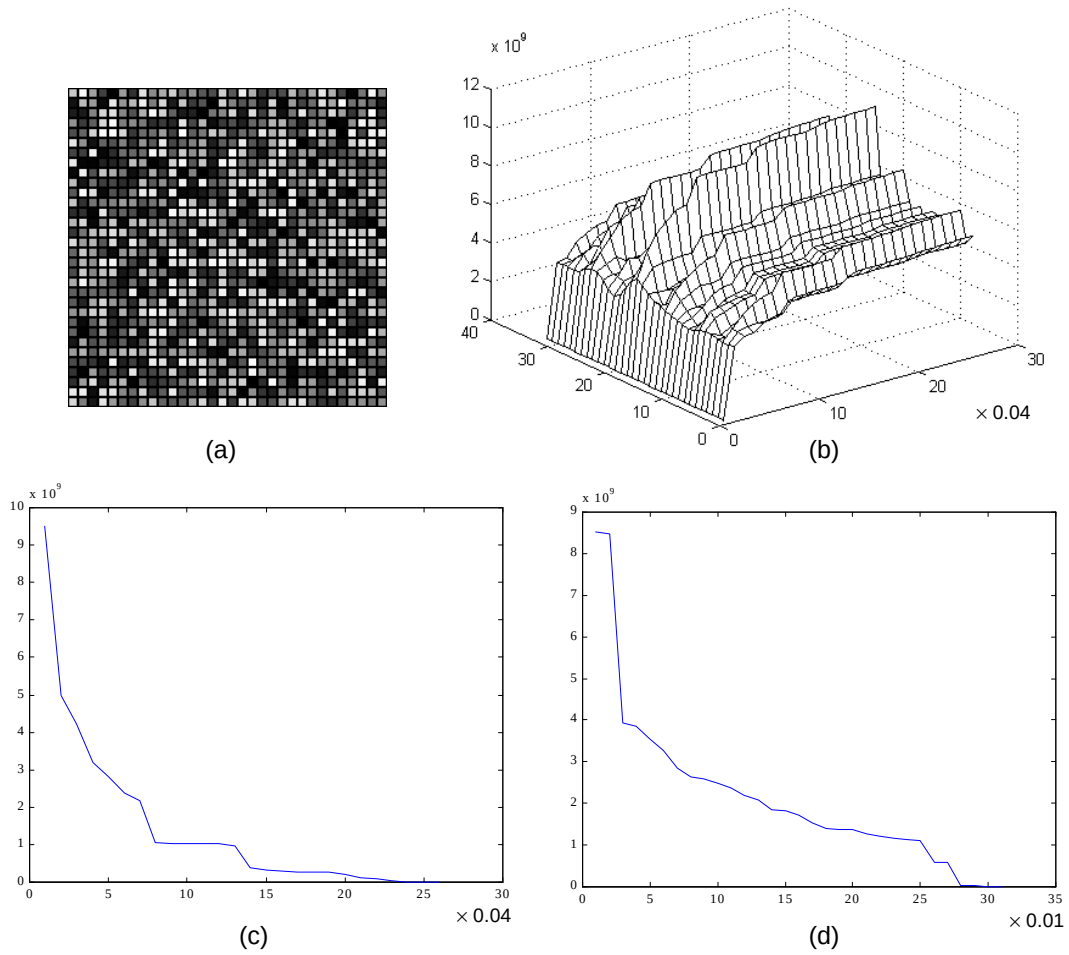

Figure 8. Degradation in summation accuracy due to AO plane filtering: (a) a random-valued 32×32 LCD panel image; (b) simulated output vector values plotted against interaction heights in the range $[0, 1]$ with graduations of 0.04; (c) highest error in each vector; (d) highest error in each vector over a smaller range $[0.0, 0.3]$ with graduations of 0.01.

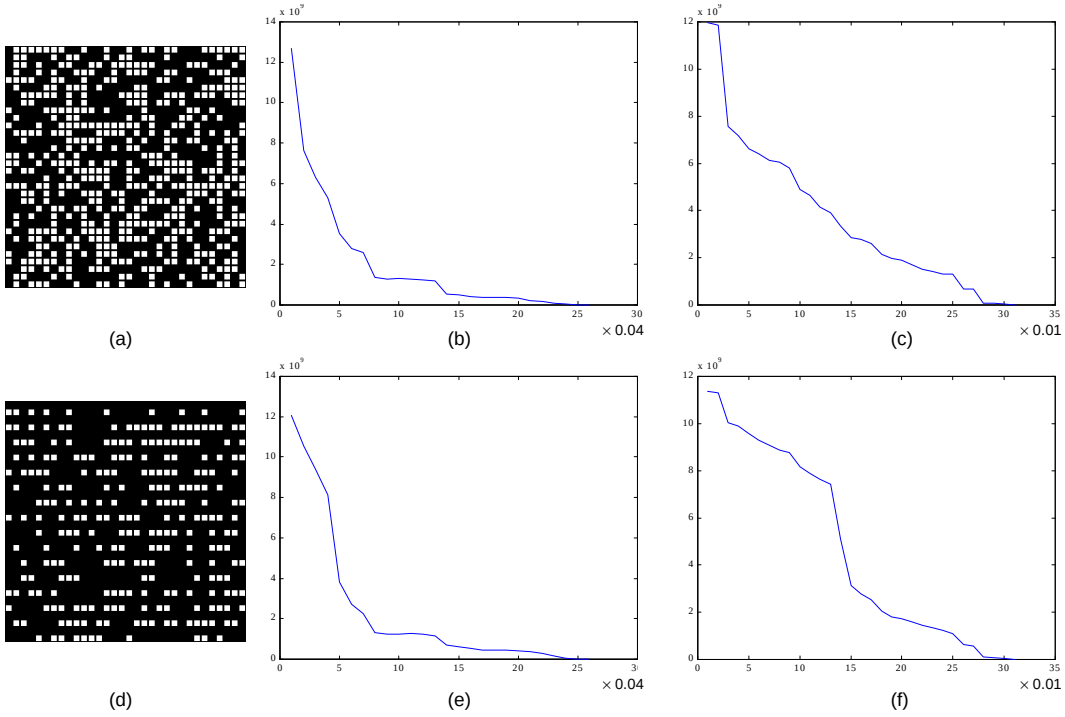

Figure 9. Degradation in summation accuracy due to AO plane filtering: (a) and (d) two binary LCD panel images; (b) and (e) respective vector error against interaction height in the range $[0, 1]$; (c) and (f) respective vector error against interaction height in range $[0.0, 0.3]$.

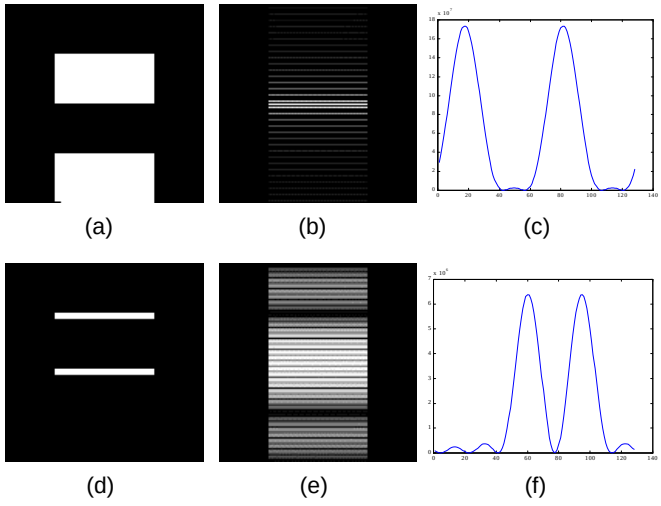

Figure 10. Required inter-row spacing in the input matrix grows linearly with increased resolution for a constant acoustic beam height: (a) a 4×4 input matrix; (b) corresponding AO plane signal. The minimum interaction height that resolved the two rows was determined to be 0.06; (c) the output vector after filtering at 0.06, showing clearly separated rows; (d) increasing resolution to a 32×4 matrix. As shown, a minimum of 8 rows of additional spacing was required to clearly resolve both rows in the output plane when 0.06 filtering was applied; (e) and (f) unfiltered AO plane signal and filtered output plane signal for (d), respectively.